

Estimating microstructural properties of a biomimetic tumour tissue phantom using diffusion-weighted MRI

Damien J McHugh^{1,2}, Fenglei Zhou^{1,3}, Penny L Hubbard Cristinacce^{1,2}, Josephine H Naish^{1,2}, and Geoff J M Parker^{1,2}

¹Centre for Imaging Sciences, The University of Manchester, Manchester, United Kingdom, ²Biomedical Imaging Institute, The University of Manchester, Manchester, United Kingdom, ³Materials Science Centre, The University of Manchester, Manchester, United Kingdom

Target audience: Those interested in microstructural modelling and phantom validation for diffusion-weighted MRI in oncology.

Purpose: Physical phantom experiments allow validation of microstructural models that seek to link the diffusion signal to specific tissue properties, and provide standard measurements for calibration and comparison of scanners in multi-site research¹. We have previously introduced biomimetic phantoms of axonal structure^{2,3} and here we introduce a novel phantom with microstructural characteristics mimicking tumour cellular structure. We also demonstrate how a model of the diffusion signal may be used to estimate microstructural properties of the phantom, and provide an initial assessment of the accuracy and precision of these estimates by using independent scanning electron microscope (SEM) measurements and bootstrap simulations.

Methods: Phantom construction: The phantom consists of a collection of roughly spherical polymer particles, produced by coaxial electrospraying⁴. This technique uses two polymer solutions to generate spherical core-shell structures, using polyethylene glycol for the core and polycaprolactone for the shell. Spheres were collected around a thin wire, forming a bulk sample structured as a hollow cylinder. Part of the bulk phantom was used for SEM characterisation, and part was placed in an NMR tube that was subsequently filled with cyclohexane; this sample (Fig. 1) was used for the MR experiments. **SEM characterisation:**

Ten regions of the bulk phantom were imaged with a Philips XL30 field emission gun SEM, and these images were used to measure the outer radius of the spheres. To reduce bias in choosing spheres manually, a grid was placed on each SEM image, and spheres that contained a grid intersection were chosen as potential candidates for measurement. Two perpendicular diameter measurements were made for candidate spheres that were not occluded by other neighbouring spheres, and the final size estimate was taken as the mean of these two lengths. At least 10 spheres per image were measured, and the analysis was performed independently by two observers. **MR acquisition:**

Pulsed gradient spin-echo scans were carried out on a 7 T Bruker system (Bruker BioSpin, Ettlingen, Germany), with the phantom placed inside a transmit/receive volume coil. Four separate PGSE scans were performed, each with a different diffusion time: $\Delta = 12, 25, 36, 45$ ms. For each Δ scan, images were acquired at seven gradient strengths: $G = 0, 28.5, 78.1, 119, 147, 202, 263$ mT/m, and δ was fixed at 4 ms for each scan. The lowest possible TE was chosen for each Δ to maximize signal to noise ratio (SNR), giving $TE = 21.2, 34.2, 45.2, 54.2$ ms as Δ increased. Three diffusion gradient directions were used, using a spin-echo readout with 30 mm x 30 mm FOV, 128 x 128 matrix, 1 mm slice thickness and TR=2500 ms. **MR analysis:** Mean signal intensities were obtained from the phantom ROI, and were normalised to the unweighted signal for each Δ acquisition. These signals were then fitted using a two-compartment analytic expression combining restricted diffusion inside a sphere⁵ with hindered extracellular diffusion⁶, estimating four model parameters: 'cell' radius, R (assuming negligible membrane thickness), intracellular volume fraction, f_i , free diffusivity, D , and the unweighted signal, S_0 . Three starting values were picked at random for R , f_i and D , and the fitting was repeated for each combination of these values. No constraints were applied to the fitted parameters, and the fit with the lowest value of the objective function was taken as the final result. Bootstrap-style simulations were used to assess the precision of parameter estimates. Propagation of errors was used to calculate the uncertainties on normalised signals from the phantom ROI. 95% confidence intervals, CI , were then calculated, and synthetic data sets were generated by adding or subtracting a random amount from each data point, S , such that 95% of the synthetic data points lay within $S \pm CI$. The standard deviation (SD) of the parameter estimates from fits to 10000 synthetic data sets was then calculated. The free diffusivity was also estimated directly by calculating the apparent diffusion coefficient (ADC) in the free cyclohexane, separately for each Δ acquisition.

Results and discussion: SEM characterisation: 160 spheres were measured, and both observers found the outer cell radius to be 7.9 ± 1.1 μm (mean \pm SD). An example SEM image is shown in Fig. 2, illustrating grid placement and choice of spheres. **MR experiments:** Fig. 3 shows the $b=0$ s/mm^2 image from the $\Delta=12$ ms scan, indicating the ROI used for the free cyclohexane ADC measurement and the lower signal annulus corresponding to the phantom. Cyclohexane ADC was found to be independent of Δ as expected (Fig. 4), with a mean over all directions and Δ values of $(1.36 \pm 0.03) \times 10^{-3}$ mm^2/s . For the ROI-averaged phantom signals, the highest G for $\Delta=36$ ms and the two highest G for $\Delta=45$ ms gave $\text{SNR} < 2$, and were excluded from the model fitting. The fit to the phantom data is shown in Fig. 5, where the error bars correspond to the 95% CI used in the bootstrap simulations as described above. The parameter estimates were: $R=6.1 \pm 0.9 \mu\text{m}$, $f_i=0.23 \pm 0.03$, $D=(1.40 \pm 0.09) \times 10^{-3} \text{ mm}^2/\text{s}$ and $S_0=0.994 \pm 0.009$. These parameter values come from the fit in Fig. 5, and the uncertainties are the SD of the 10000 simulation runs. The precision of the radius estimate suggests that R is lower than the outer sphere size measured using SEM. Qualitatively, this is expected given the non-zero thickness of the sphere wall, though measurements of this thickness are needed to see if this alone accounts for the difference. Modelling assumptions and/or sphere manufacturing imperfections may also contribute to the difference. The estimated free diffusivity is consistent with the free cyclohexane ADC, and the volume fraction is plausible. Work to establish a ground truth volume fraction is ongoing, which will allow the accuracy of the f_i estimate to be assessed.

Conclusion: A biophysical model was used to obtain plausible microstructural estimates from a novel biomimetic phantom. These phantoms may prove useful for testing microstructural models relevant to characterising tumour tissue, and for scanner and protocol calibration.

References: [1] Padhani et al. *Neoplasia* 2009;11:102–125. [2] Zhou et al. *ACS Appl Mater Interfaces* 2012;4:6311–6316. [3] Hubbard et al. *Magn Reson Med* 2014; doi:10.1002/mrm.25107. [4] Zhang et al. *Expert Rev Med Devices* 2012; 9:595–612. [5] Murday and Cotts. *J Chem Phys* 1968;48:4938–4945. [6] Price et al. *Biophys J* 1998;74:2259–2271. **Acknowledgements:** This work was supported by the Medical Research Council and AstraZeneca, and used facilities funded by the Biotechnology and Biological Sciences Research Council. This is a contribution from the Cancer Imaging Centre in Cambridge & Manchester, which is funded by the EPSRC and Cancer Research UK.



Fig. 1. Bulk phantom in a cyclohexane-filled NMR tube.

characterisation, and part was placed in an NMR tube that was subsequently filled with cyclohexane; this sample (Fig. 1) was used for the MR experiments. **SEM characterisation:**

Ten regions of the bulk phantom were imaged with a Philips XL30 field emission gun SEM, and these images were used to measure the outer radius of the spheres. To reduce bias in choosing spheres manually, a grid was placed on each SEM image, and spheres that contained a grid intersection were chosen as potential candidates for measurement. Two perpendicular diameter measurements were made for candidate spheres that were not occluded by other neighbouring spheres, and the final size estimate was taken as the mean of these two lengths. At least 10 spheres per image were measured, and the analysis was performed independently by two observers. **MR acquisition:**

Pulsed gradient spin-echo scans were carried out on a 7 T Bruker system (Bruker BioSpin, Ettlingen, Germany), with the phantom placed inside a transmit/receive volume coil. Four separate PGSE scans were performed, each with a different diffusion time: $\Delta = 12, 25, 36, 45$ ms. For each Δ scan, images were acquired at seven gradient strengths: $G = 0, 28.5, 78.1, 119, 147, 202, 263$ mT/m, and δ was fixed at 4 ms for each scan. The lowest possible TE was chosen for each Δ to maximize signal to noise ratio (SNR), giving $TE = 21.2, 34.2, 45.2, 54.2$ ms as Δ increased. Three diffusion gradient directions were used, using a spin-echo readout with 30 mm x 30 mm FOV, 128 x 128 matrix, 1 mm slice thickness and TR=2500 ms. **MR analysis:**

Mean signal intensities were obtained from the phantom ROI, and were normalised to the unweighted signal for each Δ acquisition. These signals were then fitted using a two-compartment analytic expression combining restricted diffusion inside a sphere⁵ with hindered extracellular diffusion⁶, estimating four model parameters: 'cell' radius, R (assuming negligible membrane thickness), intracellular volume fraction, f_i , free diffusivity, D , and the unweighted signal, S_0 . Three starting values were picked at random for R , f_i and D , and the fitting was repeated for each combination of these values. No constraints were applied to the fitted parameters, and the fit with the lowest value of the objective function was taken as the final result. Bootstrap-style simulations were used to assess the precision of parameter estimates. Propagation of errors was used to calculate the uncertainties on normalised signals from the phantom ROI. 95% confidence intervals, CI , were then calculated, and synthetic data sets were generated by adding or subtracting a random amount from each data point, S , such that 95% of the synthetic data points lay within $S \pm CI$. The standard deviation (SD) of the parameter estimates from fits to 10000 synthetic data sets was then calculated. The free diffusivity was also estimated directly by calculating the apparent diffusion coefficient (ADC) in the free cyclohexane, separately for each Δ acquisition.

Results and discussion: SEM characterisation: 160 spheres were measured, and both observers found the outer cell radius to be 7.9 ± 1.1 μm (mean \pm SD). An example SEM image is shown in Fig. 2, illustrating grid placement and choice of spheres. **MR experiments:** Fig. 3 shows the $b=0$ s/mm^2 image from the $\Delta=12$ ms scan, indicating the ROI used for the free cyclohexane ADC measurement and the lower signal annulus corresponding to the phantom. Cyclohexane ADC was found to be independent of Δ as expected (Fig. 4), with a mean over all directions and Δ values of $(1.36 \pm 0.03) \times 10^{-3}$ mm^2/s . For the ROI-averaged phantom signals, the highest G for $\Delta=36$ ms and the two highest G for $\Delta=45$ ms gave $\text{SNR} < 2$, and were excluded from the model fitting. The fit to the phantom data is shown in Fig. 5, where the error bars correspond to the 95% CI used in the bootstrap simulations as described above. The parameter estimates were: $R=6.1 \pm 0.9 \mu\text{m}$, $f_i=0.23 \pm 0.03$, $D=(1.40 \pm 0.09) \times 10^{-3} \text{ mm}^2/\text{s}$ and $S_0=0.994 \pm 0.009$. These parameter values come from the fit in Fig. 5, and the uncertainties are the SD of the 10000 simulation runs. The precision of the radius estimate suggests that R is lower than the outer sphere size measured using SEM. Qualitatively, this is expected given the non-zero thickness of the sphere wall, though measurements of this thickness are needed to see if this alone accounts for the difference. Modelling assumptions and/or sphere manufacturing imperfections may also contribute to the difference. The estimated free diffusivity is consistent with the free cyclohexane ADC, and the volume fraction is plausible. Work to establish a ground truth volume fraction is ongoing, which will allow the accuracy of the f_i estimate to be assessed.

Conclusion: A biophysical model was used to obtain plausible microstructural estimates from a novel biomimetic phantom. These phantoms may prove useful for testing microstructural models relevant to characterising tumour tissue, and for scanner and protocol calibration.

References: [1] Padhani et al. *Neoplasia* 2009;11:102–125. [2] Zhou et al. *ACS Appl Mater Interfaces* 2012;4:6311–6316. [3] Hubbard et al. *Magn Reson Med* 2014; doi:10.1002/mrm.25107. [4] Zhang et al. *Expert Rev Med Devices* 2012; 9:595–612. [5] Murday and Cotts. *J Chem Phys* 1968;48:4938–4945. [6] Price et al. *Biophys J* 1998;74:2259–2271. **Acknowledgements:** This work was supported by the Medical Research Council and AstraZeneca, and used facilities funded by the Biotechnology and Biological Sciences Research Council. This is a contribution from the Cancer Imaging Centre in Cambridge & Manchester, which is funded by the EPSRC and Cancer Research UK.

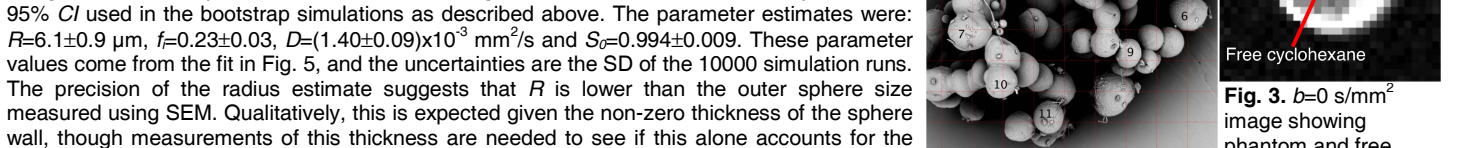


Fig. 2. One of the SEM images

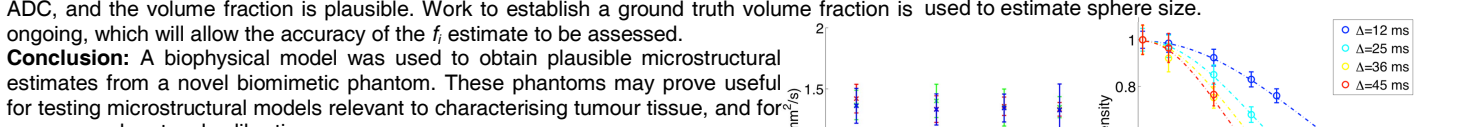


Fig. 3. $b=0$ s/mm^2 image showing phantom and free cyclohexane regions.

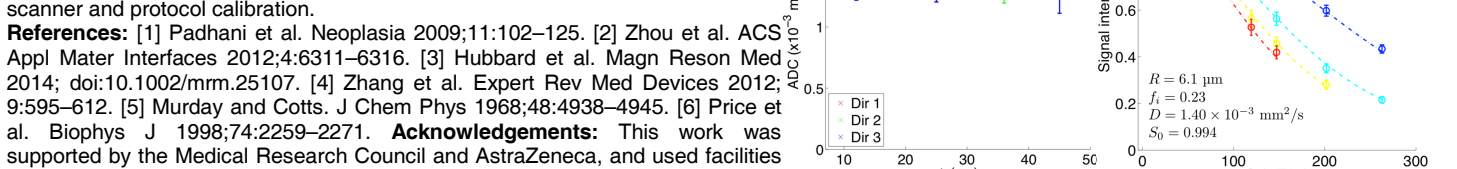


Fig. 4. Free cyclohexane ADC as a function of Δ .



Fig. 5. Phantom ROI signals as a function of G & Δ , and fit to model.